

BEHAVIOUR OF PULSE LOADED PLATES AT GREAT DEFORMATIONS

V.B. Yudaev, V.M. Favorin*

Theoretical and experimental investigation of thin plate behaviour at great deformations subjected to dynamic loads is given. A mathematical model is obtained to study buckling of the shell. Plate dynamic failure and buckling are found to occur much later than at static loading. The problems are solved numerically (using the finite difference method). The experimental part is based on the high speed filming method.

INTRODUCTION

One of the advantages of the dynamic processes is the possibility to control the plate or rod behaviour during deformation which allows to achieve the optimal stress-strain state. The governing factors are the pulse magnitude and shape, the area of its application to the billet etc.. Control is performed through inertial and wave mechanism at high speed deformation.

DYNAMIC DEFORMATION MODELS

Theoretical analysis is based on numerical methods of solution of differential equations of dynamic equilibrium:

$$\begin{aligned} \frac{\partial}{\partial S} [N_{\theta} \tau \cos \theta] - \frac{\partial}{\partial S} [Q_{\theta} \tau \sin \theta] - N_{\psi} + \tau (P_{\tau} - F_{\tau}) - \tau m \frac{\partial^2 \tau}{\partial t^2} &= 0 \\ \frac{\partial}{\partial S} [N_{\theta} \tau \sin \theta] + \frac{\partial}{\partial S} [Q_{\theta} \tau \cos \theta] + \tau (P_z - F_z) - \tau m \frac{\partial^2 z}{\partial t^2} &= 0 \\ \frac{\partial}{\partial S} [M_{\theta} \tau] - M_{\psi} \cos \theta &= \tau Q_{\theta} \end{aligned} \quad (1)$$

* Moscow Aviation Institute, USSR.

where r, z, s are the element cylindrical coordinates; Q - is the slope angle to axis; $N_{\theta}, N_{\varphi}, Q_{\theta}$ are normal and shear forces; M_{θ}, M_{φ} are bending moments; m is the shell mass density; P_z, P_r are external pressure components; F_r, F_z are friction force components; K is the dynamic friction coefficient. The system is completed with equations expressing displacement-strain, strain-stress, stress force and stress-moment relations as well as boundary conditions. The numerical experiment based on the finite difference method and explicit time integration allows to determine the distribution of stresses and strains in any part or pre form section at any given time. Thus failure or buckling of a structural component is predicted. Fig. 1. shows the behaviour and place of failure of an originally circular plate with an orifice as a result of impulse loads applied to the entire area and peripherally. The investigation of the dynamic shell stability requires a study of nonaxisymmetric displacement in the O circular coordinate. The shell element can rotate about the meridian by the angle φ . As in some cases it is sufficient to know the initial stage of the buckling the following set of equations could be used:

$$m \frac{\partial^2 u}{\partial t^2} = \frac{1}{r_0^2} [N_{\theta,0} + M_{\theta,0} \frac{\partial \theta_0}{\partial s}] \frac{\partial^2 u}{\partial \Phi^2} + [N_{\theta,0} - Q_{\theta,0} \frac{\partial u}{\partial s}] \frac{\partial^2 u}{\partial s^2} + \frac{1}{r_0^2} \frac{\partial^2 M_{\varphi}}{\partial \Phi^2} -$$

$$- \frac{1}{r_0^2} \left(\frac{\partial^2 u}{\partial \Phi \partial s} \frac{\partial u}{\partial s} + \frac{\sin \theta_0}{r_0} \frac{\partial u}{\partial \Phi} \right) \frac{\partial M_{\varphi}}{\partial \Phi} + \frac{M_{\theta,0}}{r_0^2} \cdot \frac{\partial}{\partial \Phi} \left[\frac{\partial^2 u}{\partial s^2} \frac{\partial u}{\partial \Phi} \right] +$$

$$+ \left(\frac{1}{r_0} \frac{\partial}{\partial s} [N_{\theta,0} \cdot r_0] - Q_{\theta,0} \frac{\partial \theta_0}{\partial s} \right) \frac{\partial u}{\partial s} + f(s, \Phi, t) \quad (2)$$

where u, f are the deviation of the nonaxisymmetric displacement and loading from the corresponding axisymmetric one which has the "o" subscript.

The loading was done by impulse magnetic field. Fig. 2 shows the behaviour and buckling and failure time of a cone mounted circular plate, as registered by high-speed filming. The greater impulse made buckling occur at $86 \cdot 10^{-6}$ s instead of 66 s, the failure occurring at $90 \cdot 10^{-6}$ s.

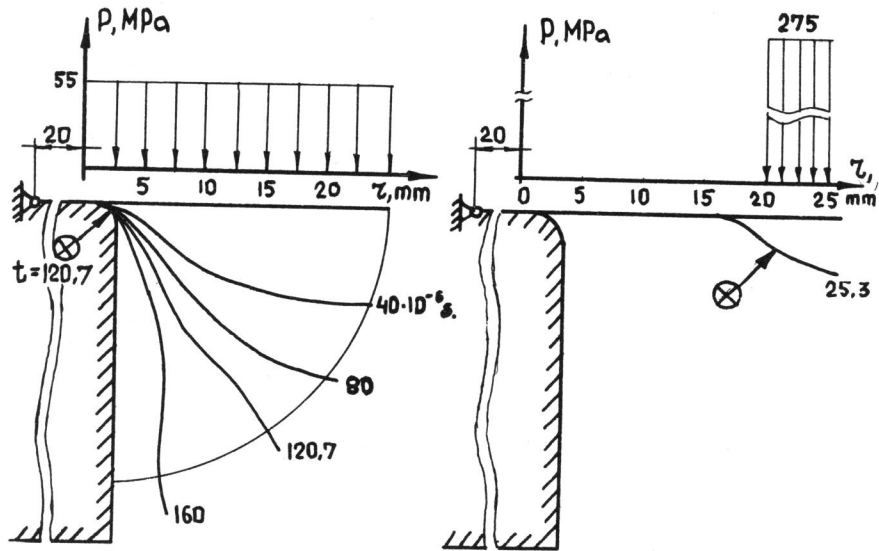


Figure 1 Pulse instantaneous position, magnitude and shape during the circular plate deformation

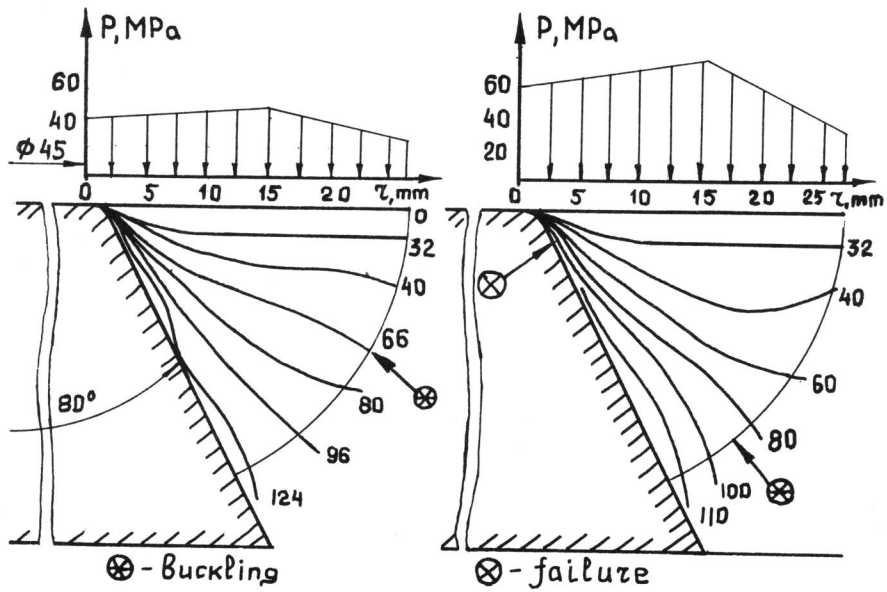


Figure 2 Circular plate behaviour and failure related to impulse localization